

STABILITY AND TRANSITION COMPUTATIONS FOR COMPLEX BASIC FLOWS

D. Arnal - G. Casalis - Ch. Airiau - F. Cazenave
CERT/ONERA-DERAT - 2 avenue E. Belin - 31055 TOULOUSE Cedex, France

Abstract

The classical linear stability theory of a laminar boundary layer flow is coupled together with the so-called e^n method in order to predict transition location. Classical use of this technic is done with boundary layer calculation but in some complex cases, the main flow needs to be calculated by solving the steady Navier-Stokes equations. This paper is devoted to the analysis of three examples of such cases. The first one deals with an isolated small bump placed on a flat plate. In the second one, a classical ONERA D airfoil is considered. In both cases, transition occurs near separation. With the third example, the effect of a leading edge bluntness in supersonic flow is studied. Finally, in these three cases, comparisons with experimental results are given.

Introduction

The subject of laminar-turbulent transition is of considerable practical interest and has a wide range of engineering applications, due to the fact that transition controls the evolution of important aerodynamic quantities such as drag or heat transfer. In a low-disturbance environment and on a smooth surface, the first step of the transition process is the so-called boundary layer receptivity, that causes the free stream fluctuations to enter the boundary layer and to generate unstable waves. The linear amplification of these waves constitutes the second step of the transition process, and it is described by the linear stability theory. The third stage occurs when wave/wave interactions and higher order instabilities develop. This non linear evolution results in the breakdown to turbulence with the first occurrence of turbulent spots.

It is clear that a rigorous modelling of such a sequence of complicated phenomena appears to be a very difficult task : the detailed characteristics of the free stream disturbances are not very well known in many cases, the receptivity theories cannot be used routinely for practical purposes and many aspects of the non linear stages are still unclear. In spite of this negative situation, transition predictions must be made. For this purpose, the most popular tool is the e^n method, that is based on linear stability theory only. Stability computations require the knowledge of the mean (or basic) flow field,

which is often obtained from boundary layer computations. In some complex cases, however, the basic flow needs to be calculated by solving the steady Navier-Stokes equations. The objective of this paper is to describe three series of numerical results dealing with such complex configurations : two-dimensional bump on a flat plate, separation bubble on a wing, leading edge bluntness effect at supersonic speeds. The study is restricted to two-dimensional mean flows.

Principle of the stability computations

Any fluctuating quantity r' (velocity, pressure, density or temperature) is expressed by :

$$r' = r(y) \exp [i(\alpha x + \beta z - \omega t)] \quad (1)$$

In the present computations, ω and β are real numbers and $\alpha = \alpha_r + i\alpha_i$ is a complex number. Depending on the sign of α_i , the disturbances are damped ($\alpha_i > 0$), neutral ($\alpha_i = 0$) or amplified ($\alpha_i < 0$).

The principle of the e^n method is well known : for a given frequency, the total amplification rate is given by :

$$\ln(A/A_0) = \int_{x_0}^x \alpha_i dX \quad (2)$$

A is a measure of the wave amplitude, and the index 0 refers to the streamwise position where the wave becomes unstable. After the total growth rate has been computed for several frequencies, it is possible to define an envelope curve which is denoted as n . With a low disturbance environment, it is assumed that transition occurs as soon as the n factor reaches a critical value in the range 7-10, i.e. when a given frequency is amplified by a factor e^7 to e^{10} .

For the first two series of computations (two-dimensional bump and separation bubble), the flow is incompressible and the computations were performed with the COCIP code developed at CERT (1). As the most "dangerous" disturbances are two-dimensional, β is set equal to 0 in relation (1). For the third case (bluntness effect at high speeds), oblique waves need to be taken into account. The so-called envelope strategy is used : at each streamwise location, the disturbance growth rate is

calculated as a function of the propagation direction $\psi = \tan^{-1}(\beta/\alpha_r)$ in order to determine the most unstable direction ψ_M . The integration (2) is then performed with the values of $\alpha_{iM} = \alpha_i(\psi_M)$. The CASTET code, also developed at CERT (2), was used for these computations.

Two-dimensional bump on a flat plate

For the stability analysis of a laminar boundary layer developing on a given body, most of the time, the surface of this body is assumed to be strictly flat, without bump or inhomogeneities. But in practise, the geometry is of course less regular, evaluations of these imperfections appear therefore necessary. Fage (3) made some fundamental experiment concerning isolated two-dimensional bumps, localized on a flat plate. The bump is symmetrical and its shape has an analytical expression (cubic curve). Different heights h of the bump were tested, but in all cases, h has an order of magnitude which is comparable to the boundary layer thickness and the slope along the bump is always smaller than 5° with respect to the flat plate. Some calculations have been done by Cebeci and Egan (4); similar experiments were performed at CERT (5) and corresponding calculations were done (6). In (3), (4), (6), the bump is localized at x close to 0.5 m; in (5), x is close to 0.3 m. In the following, the flow is assumed to be two-dimensional and incompressible.

Steady flow

For large values of the height h and for large free stream velocities, separation occurs in the rear part of the bump. A Navier-Stokes code (7) was used in order to determine the steady flow. A typical result is shown in figure 1

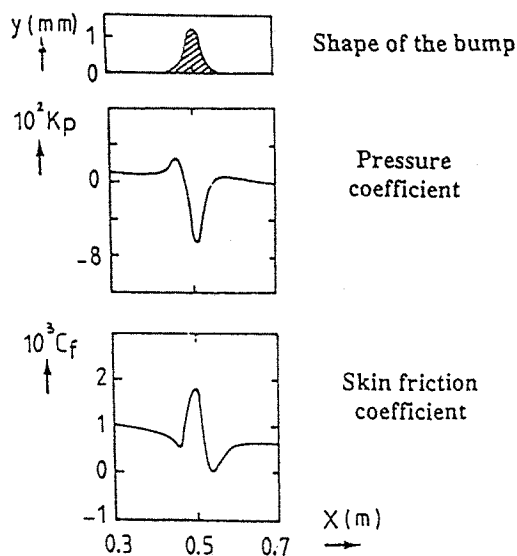


fig.1 Steady flow calculation around the bump

The flow is accelerated in the first part of the bump and decelerated in the rear part. In this example, the flow is very close to separation as it can be noted in the C_f evolution. With hot-wire measurements (5), main velocity profiles have been obtained along the bump, a comparison with a numerical result is given on figure 2.

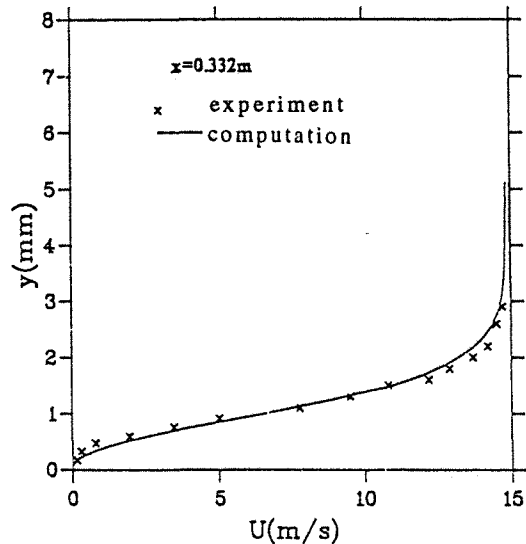


fig.2 - Comparison between experiment and Navier-Stokes calculation.

It corresponds to a x position just behind the top of the bump : just before separation. In this case, the shape factor $H = \delta_1/\theta$ is rather high, close to 4; it follows that the flow is very unstable.

Stability analysis

Classical Orr-Sommerfeld theory is then used and, in terms of the e^n method, N factors are calculated for different frequencies. Figure 3 shows a typical result for

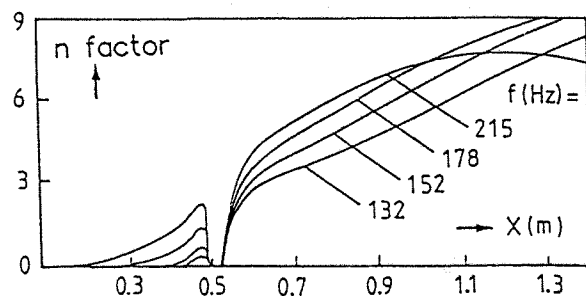


fig.3 - Stability computation around the bump. the conditions of figure 1 : the flow becomes unstable before the bump, but is still laminar; the acceleration

has a strong and complete stabilizing effect. But, just after the top, high frequency Tollmien-Schlichting waves exhibit a very rapid increase. For high values of U_e and of the height h , transition can be fixed in this rear part of the bump. Even in this extreme case, it has been possible to determine experimentally an N factor for different frequencies (5). A result is given on figure 4 in

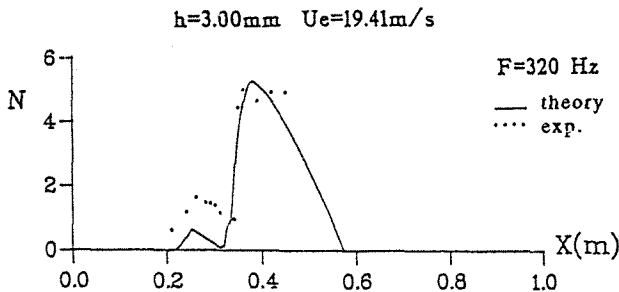


fig.4 - Comparison between experiment and stability computation.

comparison with linear stability theory. The agreement seems to be very satisfactory, except the final decrease of the theoretical value, but this one is not physical : transition occurs at $x/c \approx 0.35$ m. Finally, concerning the transition location, the following table summarizes the results obtained in (4), the original experimental results of Fage (3) and our present results :

U_e (m/s)	h (mm)	x_T (Cebeci)	x_T (CERT)	x_T (Fage)
25.1765	0.7874	1.37	1.24	1.39
21.153	1.3335	1.17	1.16	1.39
23.7744	1.3335	0.82	1.05	1.14
28.956	1.3335	0.64	0.91	0.89

Transition is theoretically estimated when the n factor reaches the value $n_T = 8.4$. Despite this difficult configuration (rapid x variation of the mean flow, separation), the overall agreement is acceptable. One of the conclusions of this study is the following : the bump is symmetrical, when U_e and h are not too large, stabilizing and destabilizing effects are more or less comparable, but for large values, symmetry is broken : transition can occur in the adverse pressure gradient region. Furthermore, in that case, the frequencies of the most amplified instability waves are higher than those which correspond to the flat plate case and, as demonstrated in (5), even the phenomenology in the transition regime is not the same. "High frequency transition" takes place instead of the classical spots appearance. Is that a general feature of inflexional

instability in comparison with the flat plate viscous instability ?

Separation bubble on a two-dimensional wing

Experiments were carried out at CERT (8) on a two-dimensional ONERA D wing. The model was placed without incidence in a wind tunnel, the test section of which was 300 mm x 400 mm. The chord of the profile was 200 mm, the potential flow velocity, 24 m/s with a free stream turbulence level equal to 0.3 %. Laminar-turbulent transition was found to occur between $x/c = 0.8$ and $x/c = 0.9$. According to the classical procedure of linear stability theory, the first task is to calculate the steady main flow.

Calculation of the steady main flow

Using the experimental values of the pressure coefficients, a boundary layer calculation showed that a separation occurred at $x/c \approx 0.72$, in the laminar region. Therefore, like for the previous case of the bump on the flat plate, it was necessary to solve the steady two-dimensional Navier-Stokes equations written for an incompressible flow. This code has been developed by de Saint Victor (9). The primitive variables are used in a staggered mesh, the scheme is implicit and a SIMPLE-like procedure is implemented. For the example given on figure 5, there are 110 points on each side of the wing

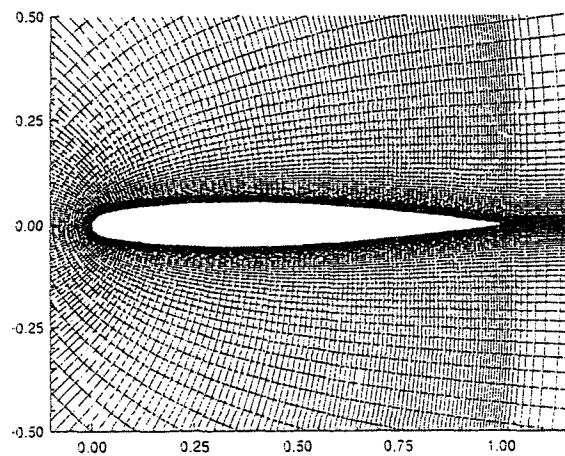


fig.5 - ONERA D airfoil : mesh for the Navier-Stokes computation.

and around 30 points in the boundary layer. Transition location is fixed at $x/c \approx 0.83$ and a simple algebraic turbulence model is used for $x/c > 0.83$. An example of

results is given on figure 6. Displacement thickness δ_1

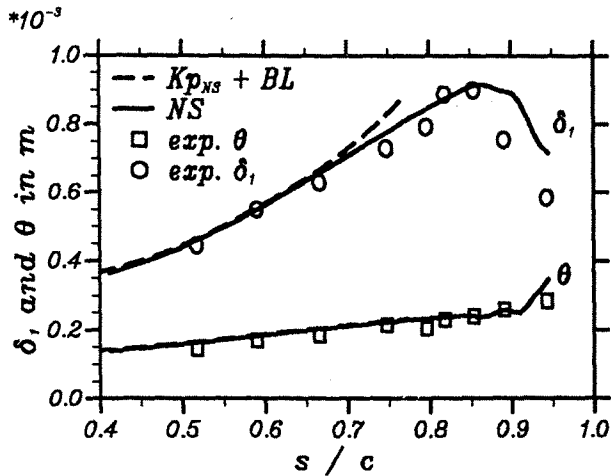


fig. 6 - Displacement thickness and momentum thickness : comparison between computation and experiment

and momentum thickness θ are represented as functions of the curvilinear s/c position. Four results are represented. The symbols come from experiment. The dashed line corresponds to a laminar boundary layer calculation with the calculated (Navier-Stokes) K_p distribution, separation occurs at $s/c \approx 0.76$. The dotted line and the full line represent Navier-Stokes calculation with two different meshes. The agreement is very satisfactory as illustrated by the decrease of δ_1 at transition. Other results can be found in (10). Finally, at each station in x , the flow is calculated with respect to the following axis : the first one is tangent to the wing, the other one is normal to it. Let us write (U, V) the two corresponding components of the velocity.

Stability analysis

Two different theories are compared. The classical one uses the parallel flow approximation by neglecting the vertical component V of the main profile. The fluctuation is searched under the normal mode (1). The second theory is the so-called PSE approach, proposed in 1987 by Herbert (11). Non parallel effects are taken into account : the V component is no longer neglected and the fluctuation has a generalized form :

$$u(x,y,t) = u(x,y) e^{i \left(\int_{x_0}^x \alpha(\xi) d\xi - \omega t \right)}$$

The wave number α is complex and has a weak dependence on x as well as the amplitude function $u(x,y)$. In both theories, ω is real. The first approach leads to an eigenvalue problem, the second one to a system of partial differential equations, which is parabolic in x .

In the two described fluctuation forms, the imaginary part of α represents a growth rate, defining thereby the

amplification of the disturbances $\text{Ln} \frac{A(x,f)}{A_0(f)}$ given by (2) which depends on x and on f , the physical frequency, linked to ω . In terms of the classical e^n method, we write $N(x,f) = \text{Ln} \frac{A(x,f)}{A_0(f)}$, where A_0 is the amplitude of the perturbation at the neutral curve. In the linear theory, A_0 does not have to be fixed. The $N(x,f)$ factor depends on the frequency ; varying this latter, the most amplified case has been found to correspond to $f = 1000$ Hz. This is in agreement with experimental measurements (8). Figure 7 represents four different results for $f = 1000$ Hz. There are two different calcul-

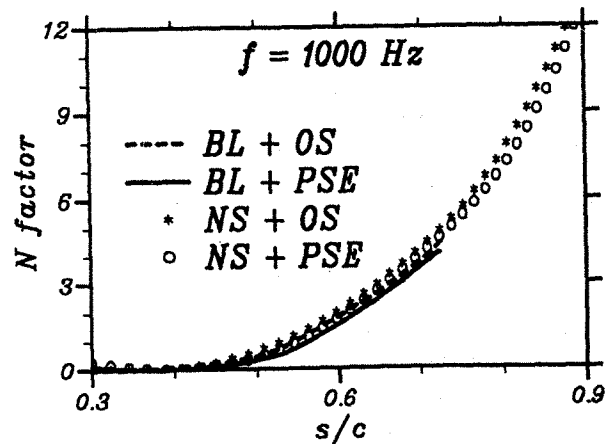


fig. 7 - Stability computations comparison

ations of the main flow : boundary layer (BL) and Navier-Stokes (NS) and two different stability approaches : Orr-Sommerfeld (OS) and the second one (PSE). The two curves with the BL calculation stop at $s/c \approx 0.74$ (let us recall that separation occurs at $x/c \approx 0.72$). We can firstly remark that, up to $s/c \approx 0.74$, BL and NS are in very good agreement with respect to stability analysis which is really a fine test. Secondly the PSE approach can be applied for complex flows, possibly with separation. Thirdly, non parallel effects, measured with the differences between OS and PSE, are small. As shown in (10), this result is a general one for two-dimensional flows. Non parallel effects seem to become more important already with oblique waves and more generally with three-dimensional flows.

Effect of leading edge bluntness in supersonic flow

The effect of nose bluntness on transition at high speed has been studied by many investigators due to its importance for many hypersonic configurations. Stetson et al (12), for instance, studied the transition mechanisms on blunt cones at a free stream Mach number equal to 8. One of the main results was that transition location

moved downstream for small values of the nose radius. Malik et al (13) performed a linear stability analysis for these experiments. By using the e^n method, it was found that the predicted transition Reynolds number increased due to small nose bluntness, in qualitative agreement with Stetson's measurements.

The results presented in this paragraph are related to the analysis of the bluntness effects for flat plates at Mach 3.5. The details of the computations are given in (14).

Mean flow computations - Numerical difficulties

The computations were carried out for a sharp leading edge and for blunt leading edges with a small radius r . In order to properly calculate the entropy layer effects, the compressible Navier-Stokes equations are solved in a small region including the subsonic zone around the leading edge. Further downstream, the mean flow field is deduced from PNS (Parabolized Navier-Stokes) calculations. The numerical codes were developed at CERT by Lafon (15).

It is well known that the numerical accuracy of the mean flow results must be extremely high, because the stability results will be very sensitive to any small departure from the "exact" flow field. Inaccuracies of the stability results arise particularly when the instability is inflectional. In this case, the growth rate depends on two parameters : the height y_S of the generalized inflection point and the value of $\rho dU/dy$ at this point. It follows that the basic flow calculations need to be very accurate in the neighbourhood of y_S , especially when this point is located far from the wall -as it is the case at supersonic speeds. To illustrate this problem, figure 8 compares the n factors obtained from two mean flow computations, one with 50 points in the direction normal to the wall, the other with 100 points. Although there is no visible difference in the velocity and temperature profiles, the n factors differ by about 10 percent. All the results presented below were obtained with a grid having 180 points in the direction normal to the wall. About 800 points were used in the streamwise direction.

In order to reduce the computing time, the stability equations are solved from the wall to some upper limit which is smaller than the upper boundary of the mean flow calculations. A difficulty, which is linked to the use of the Navier-Stokes equations, is to define the extent of the integration domain of the stability equations in the direction normal to the wall. This problem is of major importance in the present case due to the entropy swallowing effects. It will be briefly discussed below.

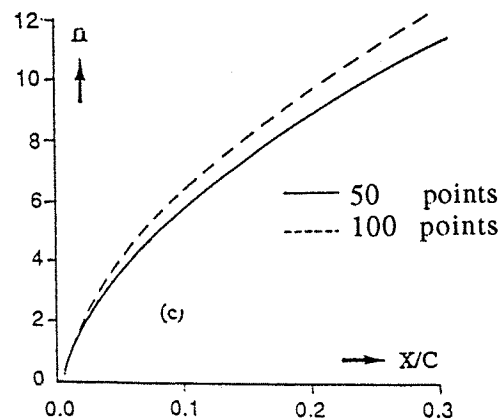
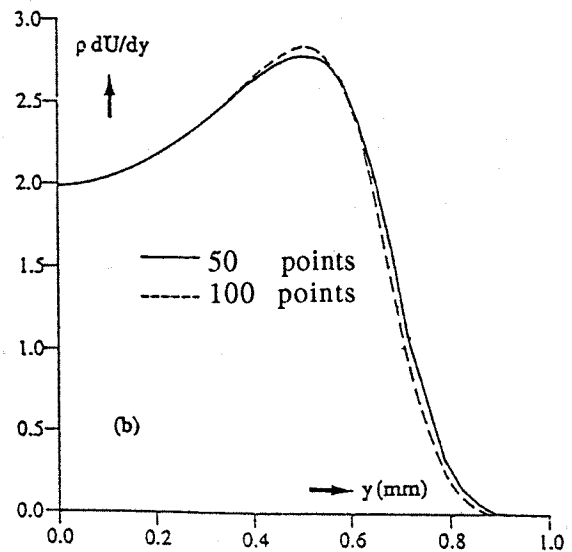
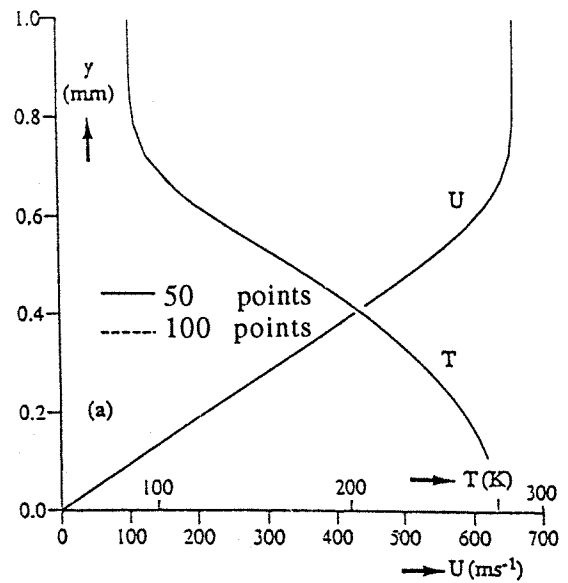


fig. 8 - Effect of the accuracy of the basic flow computations on the n factor (flat plate, Mach number = 3.5)

Results

Figure 9 shows a comparison between measured and

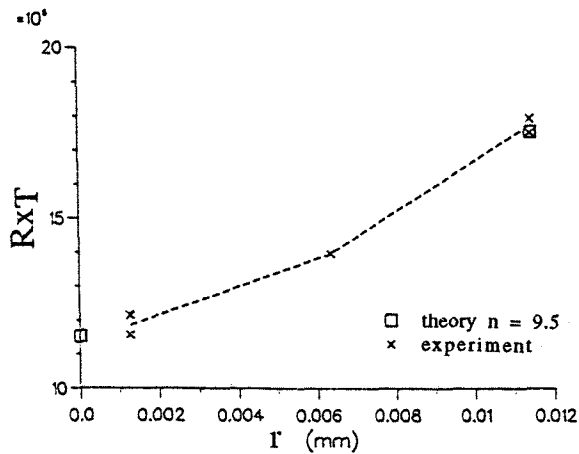


fig. 9 - Transition Reynolds number as function of the radius r. Comparison between experiment and stability computations

computed transition Reynolds numbers. The experimental data were obtained on a flat plate in the "quiet tunnel" at NASA Langley for a free stream mach number equal to 3.5 (16). The stagnation temperature and the stagnation pressure are 300 K and 11.5 bars, respectively. The wall is adiabatic. The theoretical values of R_{xT} were obtained for $n = 9.5$ and for two values of r : 0 (sharp leading edge) and 0.0114 mm. The agreement is satisfactory.

Similar computations were carried out for other values of r and other values of the stagnation pressure. The results are summarized in figure 10, which shows the evolution of R_{xT} as a function of the Reynolds number R_r formed with the leading edge radius. The open symbols correspond to $n = 7$, the full symbols correspond to $n = 9.5$. There are in fact two values of R_{xT} for the computational points associated with the three higher values of R_r . They correspond to two different heights of the integration domain of the stability equations. Although these heights differ by a factor two, the final results are close together.

The major results is that R_{xT} increases as the leading edge bluntness increases. In the experiments, however, this trend is reversed when R_r exceeds some critical value. A simple linear stability analysis cannot reproduce this behaviour.

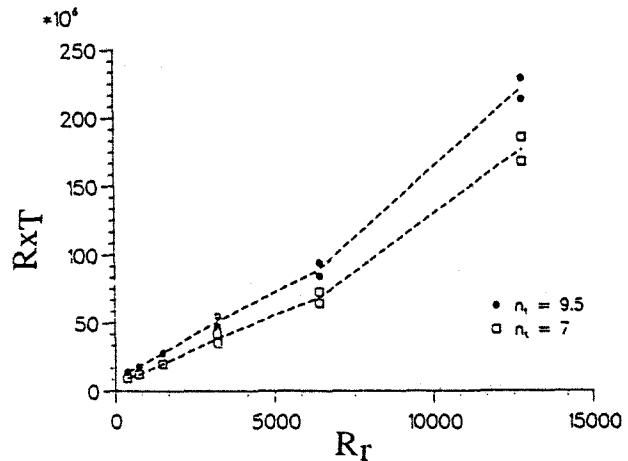


fig. 10 - Transition Reynolds number as function of bluntness Reynolds number

Conclusion

The e^n method remains the most widely used technique to estimate the transition location. In the linear regime of amplification, it is able to determine the characteristics of the unstable eigenmodes -provided the basic flow is accurate enough. It is also a very efficient tool for parametric studies: for a given test model and for a given disturbance environment, the e^n method can predict the variation of the transition location when changing a parameter which governs the linear stability properties of the flow - for instance the height of a bump or the radius of a leading edge.

However, many numerical and experimental studies pointed out the deficiencies of the e^n method: the receptivity mechanisms are not accounted for, and the non-linear phenomena are replaced by a continuous linear amplification up to the onset of transition. Clearly, the first problem is a long term issue. As far as non-linear mechanisms are concerned, the PSE represent a promising approach. But, in any case, the key problem remains to define the value of the n factor at the onset of transition.

References

- (1) G. Casalis. *Instabilités primaire et secondaire dans la couche limite laminaire pour un fluide incompressible*. Thesis, Paris VI University (1990)
- (2) D. Arnal. *Stabilité et transition des couches limites laminaires bidimensionnelles, sur paroi athermane*. La Recherche Aérospatiale, n° 1988-4 (1988)
- (3) A. Fage. *The smallest size of spanwise surface corrugation which affects boundary layer transition on an airfoil*. R&M N.2120, British A.R.C. (1943)
- (4) T. Cebeci - D.A. Egan. *The effect of wale-like roughness on transition*. AIAA Paper N° 88-0139 (1988)
- (5) F. Meininger. *Fluctuations de vitesse et de pression dans des transitions provoquées par gradient de pression, rugosité bidimensionnelle ou déformation de paroi : étude expérimentale et numérique*. Thesis ENSAE (Mars 1991)
- (6) C. Ginovart. *Transition provoquée par une bosse bidimensionnelle*. Rapport de stage ENSMA (1988)
- (7) Ch. Tenaud. *Mélange de couches limites et sillages*. Rapport de fin d'études, CERT (1984)
- (8) J. Cousteix - G. Pailhas. *Etude exploratoire d'un processus de transition laminaire-turbulent au voisinage du décollement d'une couche limite laminaire*. La Recherche Aérospatiale 1979-3
- (9) X. de Saint Victor - C. Perrin. *Calcul d'écoulements autour d'un profil d'aile bidimensionnel à nombre de Reynolds modéré*. Rapport Final DERAT n° 76/5004.44 (Juillet 1992)
- (10) Ch. Airiau. *Stabilité linéaire et faiblement non linéaire d'une couche limite laminaire incompressible par un système d'équations parabolisé (PSE)*. Thesis ENSAE (Juin 1994)
- (11) T. Herbert - F.P. Bertolotti. *Stability analysis of non parallel boundary layers*. Bull. Am. Phys. Soc., 32 (1987)
- (12) K.F. Stetson - E.R. Thompson - J.C. Donaldson - L.G. Siler. *Laminar boundary layer stability experiments on a cone at Mach 8 - Part 2 : blunt cone*. AIAA Paper 84-0006 (1984)
- (13) M.R. Malik - R.E. Spall - C.L. Chang. *Effect of nose bluntness on boundary layer stability and transition*. AIAA Paper 90-0112 (1990)
- (14) F. Cazenave. *Etude numérique des effets de l'érousement de plaques planes sur la transition en écoulement supersonique et hypersonique*. Thesis, ENSAE (1993)
- (15) A. Lafon. *Calcul d'écoulements visqueux hypersoniques*. R.T. 32/5005.22, CERT/ONERA (1990)
- (16) F.J. Chen - M.R. Malik - I.E. Beckwith. *Boundary layer transition on a cone and flat plate at Mach 3.5*. AIAA Journal, Vol. 27, N° 6 (1989)